Nanostructured zinc oxide platform for cholesterol sensor

Pratima R. Solanki,[a] Ajeet Kaushik, Anees A. Ansari, and B. D. Malhotra[b]
Department of Science and Technology Center on Biomolecular Electronics, National Physical Laboratory, Dr. K. S. Krishnan Marg, New Delhi 110012, India

(Received 27 November 2008; accepted 3 March 2009; published online 8 April 2009)

Nanostructured zinc oxide (nano-ZnO) film has been fabricated onto indium tin oxide (ITO) containing preferred (002) plane and 10 nm crystallite size using sol-gel technique for immobilization of cholesterol oxidase (ChOx). Electrochemical response of ChOx/nano-ZnO/ITO bioelectrode determined as a function of cholesterol concentration using cyclic voltammetry technique reveals improved detection range (5–400 mg/dl), low detection limit (0.5 mg/dl), fast response time (10 s), sensitivity (0.059 μA/mg dl^{-1} cm^{-2}), and low value (0.98 mg/dl) of Michaelis–Menten constant (K_m). It is shown that nano-ZnO film provides better environment and enhanced electron transfer between ChOx and electrode. © *2009 American Institute of Physics*. [DOI: 10.1063/1.3111429]

Nanostructured metal oxide films such as zinc oxide (ZnO), cerium oxide, and titanium oxide have recently attracted much attention due to their interesting optical, electrical, and molecular properties for biosensor applications.[1–3] Among these, ZnO nanostructured film due to wide band gap (3.37 eV), large excitation binding energy (60 eV), high surface area, nontoxicity, good biocompatibility, chemical stability, and high electron communication feature is preferred for development of biosensors for clinical diagnostics.[2] The high isoelectric point (IEP) of ~9.5 for ZnO is advantageous for enhanced electrostatic interaction with enzymes having low IEP.

Krishnamoorthy *et al.*[4] developed surface acoustic wave biosensor to investigate characteristics of cytokine immobilized ZnO and SiO_2 films grown onto (100) Si substrates. Wang *et al.*[5] prepared ZnO nanocombs to immobilize glucose oxidase. Zhu *et al.*[6] used ZnO nanoparticles to investigate electrochemistry of microperoxidase. Yan *et al.*[7] fabricated ZnO based acoustic resonator as mass sensor by multitarget magnetron sputtering under optimized deposition conditions. Wei *et al.*[8] utilized ZnO nanorods array for application to glucose biosensor. Meulenkamp *et al.*[9] prepared sol-gel based ZnO matrix for a mediator-free tyrosinase biosensor. The cholesterol biosensor based on rf sputtered nanoporous ZnO/Au film[2] shows high K_m, poor detection limit and is expensive. ChOx/chitosan-ZnO bioelectrode shows K_m as 0.223 mM, linearity up to 300 mg/dl and shelf life of 8 weeks.[10]

The sol-gel derived nanostructured metal oxide films due to better thermal stability, low cost, biocompatibility, nontoxicity, tunable porosity, low temperature processing, etc. have attracted much interest for biosensing application.[11] We report results of studies relating to sol-gel derived nano-ZnO film deposited onto indium-tin-oxide (ITO) substrate for application to cholesterol sensor.

Zinc acetate hydrate (1 g) is dissolved in 20 ml ethanol at 25 °C. Then 5 ml (1*M*) solution of ammonium hydroxide is added drop wise to this solution with constant stirring for 1h at 25 °C to maintain *p*H 10. A white precipitate of $Zn(OH)_2$ obtained is washed several times with de-ionized water until neutral *p*H is reached. Subsequently, dilute HNO_3 (1*M*) is added to precipitate at 60 °C to obtain a solution of *p*H 1. The resulting sol is used to fabricate thin film on ITO coated glass plate via dip coating technique and allowed to dry at 500 °C. 10 μl of ChOx [1.0 mg/ml, in phosphate buffer (PB), 50 mM, *p*H 7.0] is immobilized onto nano-ZnO/ITO film (0.25 cm^2) via physisorption and kept overnight for drying. The higher activity of ChOx/nano-ZnO/ITO bioelectrode obtained at *p*H 7.0 reveals that ChOx/nano-ZnO/ITO bioelectrode is more active at *p*H 7.0.

X-ray diffraction (XRD) [Cu $K\alpha$ radiation (Rigaku)], atomic force microscopy (AFM) (Veeco DICP2), and Fourier-transform infrared (FTIR) (Perkin-Elmer, Model 2000) studies have been conducted for characterization of nano-ZnO/ITO electrode and ChOx/nano-ZnO/ITO bioelectrode. Electrochemical studies are carried out on an Autolab potentiostat/galvanostat in PB saline (PBS) (50 mM, *p*H 7.0, 0.9% NaCl) containing 5 mM $[Fe(CN)_6]^{3-/4-}$.

Figure 1(a) exhibits XRD pattern of nano-ZnO film revealing growth of oriented nanocrystallites (estimated as 10 nm using Scherer equation) in preferred (002) reflection plane at 34.5° indicating growth along *c*-axis normal to nano-ZnO film due to presence of stress in ZnO film arising due to embedded oxygen at interstitial sites in nano-ZnO film at 500 °C.[4]

FTIR [Fig. 1(b)] of nano-ZnO film (curve a) exhibits weak bands at 3350 and 1594 cm^{-1} corresponding to O–H stretching due to physically adsorbed water on nano-ZnO film surface. 520 cm^{-1} band (curve a) arises due to oxygen deficiency and/or oxygen vacancy defect complex in ZnO.[12,13] On immobilization of ChOx onto sol-gel derived nano-ZnO, 520 cm^{-1} peak shifts to 540 cm^{-1} due to electrostatic interactions between nano-ZnO and ChOx. FTIR spectra of ChOx/nano-ZnO/ITO (curve b) exhibits bands at 3250 cm^{-1} (corresponding to N–H stretching in amide II), 1590 cm^{-1} (corresponding to C–N stretching and N–H bending modes of amide I bands), and 1000 cm^{-1} (assigned to C–O stretching) due to amide bands in protein revealing immobilization of ChOx onto nano-ZnO film via electrostatic interactions.

[a]Electronic mail: pratimasolanki@yahoo.com.
[b]Electronic mail: bansi.malhotra@gmail.com. Tel.: +91 11 45609152. FAX: +91 11 45609310.

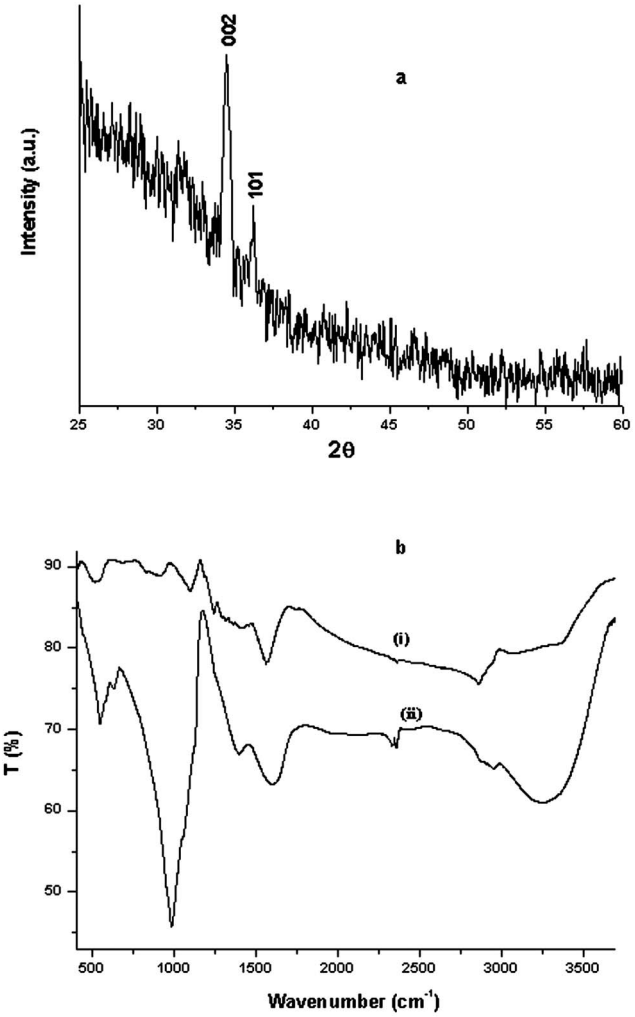

FIG. 1. (a) XRD pattern of sol-gel derived ZnO film. (b) FTIR spectra of nano-ZnO/ITO electrode (i) and ChOx/nano-ZnO/ITO bioelectrode (ii).

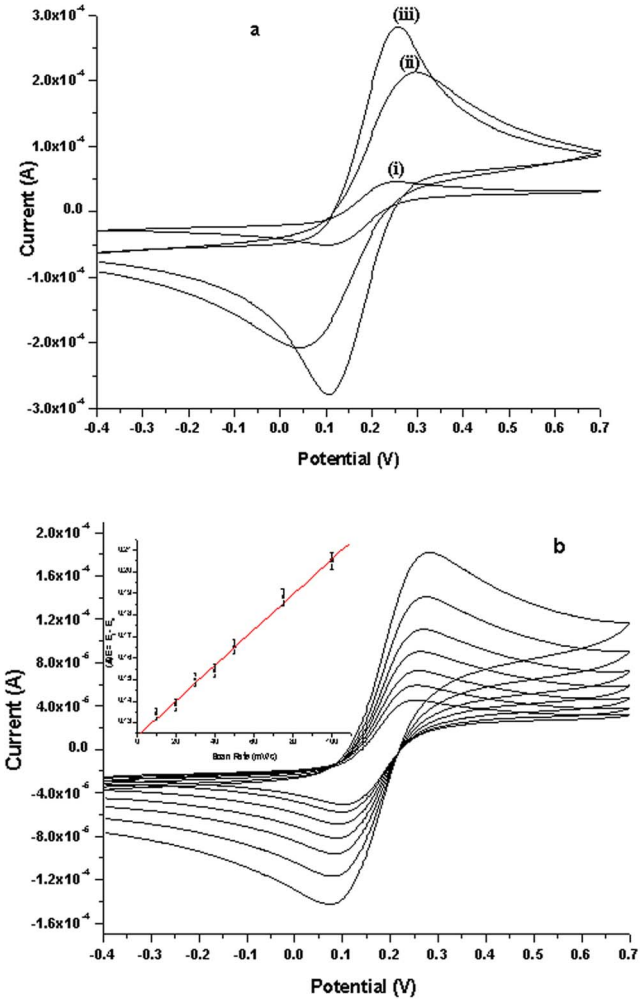

FIG. 2. (Color online) (a) Cyclic voltammogram of ITO electrode (i) nano-ZnO/ITO electrode (ii) and ChOx/nano-ZnO/ITO bioelectrode (iii). (b) Cyclic voltammogram of ChOx/nano-ZnO/ITO bioelectrode at different scan rates (10–100 mV/s). Inset is plot of potential difference vs scan rate.

AFM images (supplementary data[14]) exhibit granular nanoporous morphology of nano-ZnO/ITO electrode with surface roughness of 127 nm. However, the roughness decreases to 80 nm after ChOx immobilization onto nano-ZnO/ITO electrode revealing that nano-ZnO film provides a biocompatible environment for ChOx. Furthermore, bearing ratio plots of nano-ZnO/ITO electrode (supplementary data[14]) and ChOx/nano-ZnO/ITO bioelectrode (supplementary data[14]) show uniform surface topologies.

The results of *CV* studies [Fig. 1(a)] reveal that magnitude of current (0.21 mA) is enhanced as (curve ii) compared to that of bare ITO (curve i) revealing that nano-ZnO results in enhanced electron transport due to arrangement of ZnO molecules resulting in increased electrocatalytic surface area. The magnitude of current response further increases to 0.28 mA for ChOx/nano-ZnO/ITO bioelectrode revealing that nano-ZnO/ITO electrode provides three-dimensional platform for ChOx, resulting in enhanced electron communication between ChOx and electrode. Results of differential pulse voltammetric studies reveal similar behavior (supplementary data[14]).

The results of *CV* studies [Fig. 2(b)] of ChOx/nano-ZnO/ITO bioelectrode conducted as a function of scan rate (10–100 mV/s) reveal that peak-to-peak separation potential (ΔE, ~0.16 V) increases with increasing scan rate (inset), indicating uniform facile charge transfer kinetics and follows

$$\Delta E(V)(\text{ChOx/nano}-\text{ZnO/ITO bioelectrode}) = 0.12\ \text{V} + 0.81 \times 10^{-6}(s) \times \text{scan rate(mV/s)}\ \text{with}\ R^2 = 0.994\ldots. \quad (1)$$

The surface concentration of ionic species onto ChOx/nano-ZnO/ITO bioelectrode has been found as 1.86×10^{-8} mol cm^{-2} using[15]

$$i_p = 0.227nFAC_0^* k^0 \exp\left[\frac{-\alpha n_a F}{\text{RT}}(E_p - E_0')\right]\ldots, \quad (2)$$

where i_p is the anodic peak current, n is the number of electrons transferred (1), F is Faraday constant (96 485.34 C mol^{-1}), A is surface area (0.25 cm^2), R is gas constant (8.314 J mol^{-1} K^{-1}), C_0^* is surface concentration of ionic species onto the film surface (mol/cm^{-3}), E_p is peak potential, and E_0' is formal potential. $-\alpha n_a F/\text{RT}$ and k^0 (rate constant) corresponds to the slope and intercept of $\ln(i_p)$ versus $E_p - E_0'$ curve at a given scan rate.

Electrochemical response studies [Fig. 3(a)] of ChOx/nano-ZnO/ITO bioelectrode conducted as a function of cholesterol concentration reveal that current response increases

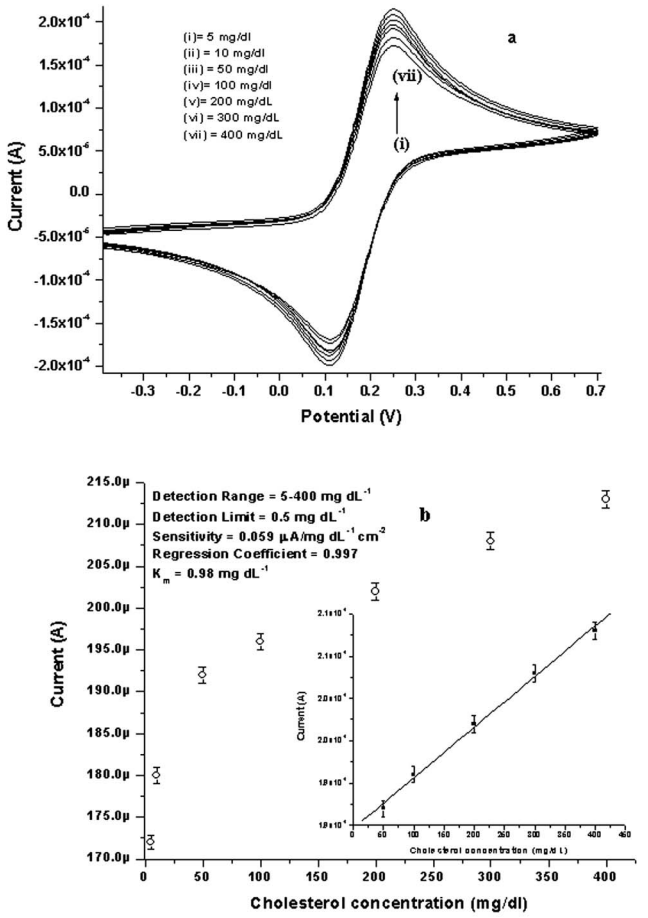

FIG. 3. (a) Electrochemical response of ChOx/nano-ZnO/ITO bioelectrode with respect to cholesterol concentration (5–400 mg/dl) at the scan rate of 20 mV s^{-1}. (b) The variation in current as a function of cholesterol concentration. Inset is linearity curve between magnitude of current vs cholesterol concentration.

with successive addition of cholesterol. This may perhaps be due to well aligned and closed packed network of nano-ZnO that acts as good accepter of electron generated during reoxidation of ChOx and transferred to electrode via Fe(III)/Fe(IV) conversion resulting in increased electrochemical current response.

The ChOx/nano-ZnO/ITO bioelectrode exhibits detection range of 5–400 mg/dl, detection limit of 0.5 mg/dl, response time of 10 s, and reproducibility of 20 times. However, good linearity is obtained in 50–400 mg/dl range with linear regression coefficient (R^2) as 0.997 [Fig. 3(b)]. The results of triplicate sets reveal reproducibility within 1%. The magnitude of current response as a function of cholesterol concentration [50–400 mg/dl, inset of Fig. 3(a)] follows

$$I_p(A)(\text{ChOx/nano} - \text{ZnO/ITO}) = 189 \times 10^{-6}(A) + 0.059 \times 10^{-6}\ \text{A dl/mg} \times \text{cholesterol concentration(mg/dl)}\ldots \quad (3)$$

The Michaelis–Menten constant (K_m) value obtained as 0.98 mg/dl using Lineweaver–Burke plot is lower than that of other metal oxide based cholesterol biosensors (supplementary data[14]).[2,3,10,14,16,17] The observed higher affinity of ChOx/nano-ZnO/ITO bioelectrode can be attributed to favorable conformation of ChOx and higher loading onto nano-ZnO film.[3] It appears that NS-ZnO/ITO film results in higher activity of immobilized ChOx molecules due to their improved conformation and orientation leading to their enhanced interaction (lower K_m) with substrate molecules resulting in low detection limit of the ChOx/NS-ZnO/ITO electrode.

The sensitivity of this ChOx/nano-Zno/ITO bioelectrode is obtained as 0.059 $\mu A/\text{mg dl}^{-1}\,\text{cm}^{-2}$ with linear regression coefficient (R^2) as 0.997. The selectivity of ChOx/nano-ZnO/ITO bioelectrode determined by measuring response current on addition of normal concentration of interferents such as ascorbic acid (AA), uric acid (UA), glucose (G), lactic acid (LA), sodium pyruvate, and urea (1) at normal concentration in blood samples [inset of Fig. 3(a)] indicates maximum interference of 4.6%. The storage stability of ChOx/nano-ZnO/ITO bioelectrode determined by measuring change in current response at regular interval of 1 week exhibits 80% response after about 3 months when stored at 4 °C.

The ChOx/nano-ZnO/ITO cholesterol biosensor has been found to have improved detection range (5–400 mg/dl), low detection limit (0.5 mg/dl), linear regression at 0.994, response time (10 s), and shelf-life (3 months). The low K_m value (0.98 mg/dl) indicates high affinity of ChOx/nano-ZnO/ITO bioelectrode to cholesterol. Efforts should be made to improve sensitivity of this electrode by controlling shape and size of nano-ZnO and to utilize this electrode for estimation of triglycerides and lipoproteins etc.

We thank Director, NPL, India for facilities. P.R.S., A.A.A., and A.K. thank CSIR, India for award of Senior Research Associate (SRA).

[1]P. R. Solanki, A. Kaushik, A. A. Ansari, G. Sumana, and B. D. Malhotra, Appl. Phys. Lett. **93**, 163903 (2008).
[2]S. P. Singh, S. K. Arya, P. Pandey, B. D. Malhotra, S. Saha, K. Sreenivas, and V. Gupta, Appl. Phys. Lett. **91**, 063901 (2007).
[3]A. A. Ansari, A. Kaushik, P. R. Solanki, and B. D. Malhotra, Electrochem. Commun. **10**, 1246 (2008).
[4]S. Krishnamoorthy, T. Bei, E. Zoumakis, G. P. Chrousos, and A. A. Iliadis, Biosens. Bioelectron. **22**, 707 (2006).
[5]J. X. Wang, X. W. Sun, A. Wei, Y. Lei, X. P. Cai, C. M. Li and Z. L. Dong, Appl. Phys. Lett. **88**, 233106 (2006).
[6]X. Zhu, I. Yuri, X. Gan, I. Suzuki, and G. Li, Biosens. Bioelectron. **22**, 1600 (2007).
[7]Z. Yan, Z. Song, W. Liu, H. Ren, N. Gu, X. Zhou, L. Zhang, Y. Wang, S. Feng, L. Lai, and J. Chen, Appl. Surf. Sci. **253**, 9372 (2007).
[8]A. Wei, X. W. Sun, J. X. Wang, Y. Lei, X. P. Cai, C. M. Li, Z. L. Dong, and W. Huang, Appl. Phys. Lett. **89**, 123902 (2006).
[9]E. A. Meulenkamp, J. Phys. Chem. B **102**, 5566 (1998).
[10]R. Khan, A. Kaushik, P. R. Solanki, A. A. Ansari, M. K. Pandey, and B. D. Malhotra, Anal. Chim. Acta **616**, 207 (2008).
[11]A. A. Ansari, P. R. Solanki, and B. D. Malhotra, Appl. Phys. Lett. **92**, 263901 (2008).
[12]J. Zheng, R. Ozisik, and R. W. Siegel, Polymer **46**, 10873 (2005).
[13]G. Xiong, U. Pal, J.G. Serrano, K.B. Ucer, R.T. Williams, Phys. Status Solidi C **3**, 3577 (2006).
[14]See EPAPS Document No. E-APPLAB-94-075913 for results of AFM, DPV studies and Table I. For more information on EPAPS, see http://www.aip.org/pubservs/epaps.html.
[15]N. Prabhakar, K. Arora, S. P. Singh, M. K. Pandey, H. Singh, and B. D. Malhotra, Anal. Chim. Acta **589**, 6 (2007).
[16]G. K. Kouassi, J. Irudayaraj, and G. McCarty, J. Nanobiotech. **3**, 1 (2005).
[17]S. Aravamudhan, A. Kumar, S. Mohapatra, and S. Bhansali, Biosens. Bioelectron. **22**, 2289 (2007).